J|A|C|S ARTICLES

Published on Web 10/16/2009

Reaction of Hydrogen or Ammonia with Unsaturated Germanium or Tin Molecules under Ambient Conditions: Oxidative Addition versus Arene Elimination

Yang Peng,[†] Jing-Dong Guo,[‡] Bobby D. Ellis,[†] Zhongliang Zhu,[†] James C. Fettinger,[†] Shigeru Nagase,*[,‡] and Philip P. Power*[,†]

Department of Chemistry, University of California, Davis, One Shields Avenue, Davis, California, 95616, and Department of Theoretical and Computational Molecular Science, Institute for Molecular Science, Okazaki, Aichi 444-8585, Japan

Received August 18, 2009; E-mail: pppower@ucdavis.edu; nagase@ims.ac.jp

Abstract: The reactions of hydrogen or ammonia with germylenes and stannylenes were investigated experimentally and theoretically. Treatment of the germylene $GeAr^{\#}_2$ ($Ar^{\#} = C_6H_3$-2,6-(C_6H_2-2,4,6-Me_3)$_2$) with H_2 or NH_3 afforded the tetravalent products $Ar^{\#}_2GeH_2$ (**1**) or $Ar^{\#}_2Ge(H)NH_2$ (**2**) in high yield. The reaction of the more crowded $GeAr'_2$ ($Ar' = C_6H_3$-2,6-(C_6H_3-2,6-$^iPr_2$)$_2$) with NH_3 also afforded a tetravalent amide $Ar'_2Ge(H)NH_2$ (**3**), whereas with H_2 the tetravalent hydride $Ar'GeH_3$ (**4**) was obtained with Ar′H elimination. In contrast, the reactions with the divalent Sn(II) aryls did not lead to Sn(IV) products. Instead, arene eliminated Sn(II) species were obtained. $SnAr^{\#}_2$ reacted with NH_3 to give the Sn(II) amide $\{Ar^{\#}Sn(\mu\text{-}NH_2)\}_2$ (**5**) and $Ar^{\#}H$ elimination, whereas no reaction with H_2 could be observed up to 70 °C. The more crowded $SnAr'_2$ reacted readily with H_2, D_2, or NH_3 to give $\{Ar'Sn(\mu\text{-}H)\}_2$ (**6**), $\{Ar'Sn(\mu\text{-}D)\}_2$ (**7**), or $\{Ar'Sn(\mu\text{-}NH_2)\}_2$ (**8**) all with arene elimination. The compounds were characterized by ^1H, ^{13}C, and ^{119}Sn NMR spectroscopy and by X-ray crystallography. DFT calculations revealed that the reactions of H_2 with EAr_2 (E = Ge or Sn; Ar = $Ar^{\#}$ or Ar′) initially proceed via interaction of the σ orbital of H_2 with the 4p(Ge) or 5p(Sn) orbital, with back-donation from the Ge or Sn lone pair to the H_2 σ^* orbital. The subsequent reaction proceeds by either an oxidative addition or a concerted pathway. The experimental and computational results showed that bond strength differences between germanium and tin, as well as greater nonbonded electron pair stabilization for tin, are more important than steric factors in determining the product obtained. In the reactions of NH_3 with EAr_2 (E = Ge or Sn; Ar = $Ar^{\#}$ or Ar′), the divalent $ArENH_2$ products were calculated to be the most stable for both Ge and Sn. However the tetravalent amido species $Ar_2Ge(H)NH_2$ were obtained for kinetic reasons. The reactions with NH_3 proceed by a different pathway from the hydrogenation process and involve two ammonia molecules in which the lone pair of one NH_3 becomes associated with the empty 4p(Ge) or 5p(Sn) orbital while a second NH_3 solvates the complexed NH_3 via intermolecular N−H···N interactions.

Introduction

The reaction of small, saturated molecules with molecular main group species under ambient conditions is a rapidly expanding research field. Several main group derivatives, which include the alkyne analogues Ar′EEAr′(E = Ge or Sn, Ar′= C_6H_3-2,6-(C_6H_3-2,6-Pr^i_2)$_2$),[1,2] stable carbenes,[3] phosphinoboranes,[4] stannylenes,[5] and low-valent group 13 metal species[6] have now been shown to react directly with H_2 under mild conditions. Stephan and his group have shown that, by use of the frustrated Lewis pair concept[7] in various phosphine-borane complexes, the activation of H_2 can be effected reversibly near room temperature.[8,9] In addition, several other H_2 activation systems, incorporating frustrated Lewis pair−borane complexes of carbenes,[10,11] amines,[12] and phosphines[13,14] have been

[†] University of California.
[‡] Institute for Molecular Science.

(1) Spikes, G. H.; Fettinger, J. C.; Power, P. P. *J. Am. Chem. Soc.* **2005**, *127*, 12232.
(2) Peng, Y.; Brynda, M.; Ellis, B. D.; Fettinger, J. C.; Rivard, E.; Power, P. P. *Chem. Commun.* **2008**, *45*, 6042.
(3) Frey, G. D.; Lavallo, V.; Donnadieu, B.; Schoeller, W. W.; Bertrand, G. *Science* **2007**, *316*, 439.
(4) Welch, G. C.; San Juan, R. R.; Masuda, J. D.; Stephan, D. W. *Science* **2006**, *314*, 1124.
(5) Peng, Y.; Ellis, B. D.; Wang, X.; Power, P. P. *J. Am. Chem. Soc.* **2008**, *130*, 12268.
(6) Zhu, Z.; Wang, X.; Peng, Y.; Lei, H.; Fettinger, J. C.; Power, P. P. *Angew. Chem., Int. Ed.* **2009**, *48*, 2031.
(7) Stephan, D. W. *Org. Biomol. Chem.* **2008**, *6*, 1535.
(8) Geier, S. J.; Gilbert, T. M.; Stephan, D. W. *J. Am. Chem. Soc.* **2008**, *130*, 12632.
(9) Ullrich, M.; Lough, A. J.; Stephan, D. W. *J. Am. Chem. Soc.* **2009**, *131*, 52.
(10) Chase, P. A.; Stephan, D. W. *Angew. Chem., Int. Ed.* **2008**, *47*, 7433.
(11) Holschumacher, D.; Bannenberg, T.; Hrib, C. G.; Jones, P. G.; Tamm, M. *Angew. Chem., Int. Ed.* **2008**, *47*, 7428.
(12) Sumerin, V.; Schulz, F.; Nieger, M.; Leskela, M.; Repo, T.; Rieger, B. *Angew. Chem., Int. Ed.* **2008**, *47*, 6001.
(13) Sumerin, V.; Schulz, F.; Atsumi, M.; Wang, C.; Nieger, M.; Leskela, M.; Repo, T.; Pyykko, P.; Rieger, B. *J. Am. Chem. Soc.* **2008**, *130*, 14117.
(14) Wang, H.; Frohlich, R.; Kehr, G.; Erker, G. *Chem. Commun.* **2008**, 5966.

 10.1021/ja9068408 CCC: $40.75

described. Bertrand and his group showed that stable carbenes could react, not only with H_2 but also with NH_3, to afford N−H bond inserted products as shown by eq 1. Experimental and theoretical work showed that the carbon substituents exerted a large effect via control of the carbene singlet−triplet energy gap, and when this gap exceeded ca. 50 kcal mol^{-1} the reaction was prevented.[3]

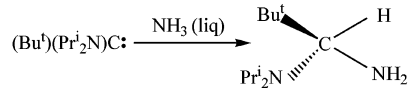

(1)

We showed recently that tin(II) carbene analogue, the diarylstannylene $SnAr'_2$, reacted with H_2, D_2, or NH_3 to give $\{Ar'Sn(\mu\text{-}H)\}_2$ (**6**), $\{Ar'Sn(\mu\text{-}D)\}_2$ (**7**), or $\{Ar'Sn(\mu\text{-}NH_2)\}_2$ (**8**) with arene elimination to give exclusively Sn(II) products (eq 2).[5]

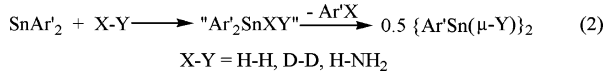

(2)

This reaction differed from that of the carbene in eq 1 where no elimination was observed. It was proposed that it proceeded via the tetravalent intermediate $Ar'_2Sn(H)X$ (X = H or NH_2) which eliminated Ar′H presumably because of the steric pressure of the two large Ar′ substituents. We have now investigated this hypothesis by changing the substituent size to relieve steric pressure. In addition we extended these studies to the lighter element germanium derivatives. We show that, in contrast to those of tin, the reactions of H_2 or NH_3 with $GeAr^#_2$ ($Ar^# = C_6H_3\text{-}2,6\text{-}(C_6H_2\text{-}2,4,6\text{-}Me_3)_2$) and $GeAr'_2$ ($Ar' = C_6H_3\text{-}2,6\text{-}(C_6H_3\text{-}2,6\text{-}{}^iPr_2)_2$) afford tetravalent products. For $GeAr^#_2$, the Ge(IV) species $Ar^#_2GeH_2$ (**1**) or $Ar^#_2Ge(H)NH_2$ (**2**) were obtained in high yield with no arene elimination. With the more crowded $GeAr'_2$, reaction with NH_3 gave the analogous Ge(IV) amido hydride $Ar'_2Ge(H)NH_2$ (**3**), whereas the Ge(IV) species $Ar'GeH_3$ (**4**) was obtained upon reaction with H_2. The reactions of the less crowded $SnAr^#_2$ with NH_3 also afforded the Sn(II) arene eliminated product $\{Ar^#Sn(\mu\text{-}NH_2)\}_2$ (**5**) whereas no reaction was observed between $SnAr^#_2$ and H_2. The very different results obtained for the germanium and tin reactions show that steric effects are of secondary importance in comparison to the electronic and bond strength differences between these two elements.

Experiment Section

General Procedures. All reactions were performed with the use of modified Schlenk techniques under anaerobic and anhydrous conditions. H_2 gas was purchased from commercial sources and was dried over a P_2O_5 column. Liquid NH_3 was dried over sodium. ^1H and $^{13}C\{^1H\}$ NMR spectra were obtained on a Varian Mercury 300 MHz spectrometer (75.5 MHz, respectively) and referenced internally to residual protio benzene or toluene in C_6D_6 or C_7D_8 solvent. Solution ^{119}Sn NMR spectra were recorded on a Varian Inova 600 MHz spectrometer (224.2 MHz) and referenced externally to neat $SnBu^n_4$. Infrared spectra were recorded as Nujol mulls between CsI plates using a Perkin-Elmer 1430 instrument. Melting points were measured in sealed glass capillaries under nitrogen by using a Mel-Temp II apparatus and are uncorrected.

$Ar^#_2GeH_2$ (1). A deep purple solution of $GeAr^#_2$[15] (0.30 g, 0.43 mmol) in toluene (50 mL) was stirred at 65 °C for 2 h under a H_2 atmosphere to give a light purple solution. The mixture was concentrated to ca. 10 mL under reduced pressure to afford colorless crystals of **1** upon cooling to ca. −16 °C. Yield: 66%. Mp: 265 °C. ^1H NMR (C_7D_8): δ 1.83 (s, 12H, *o*-CH_3), 2.26 (s, 6H, *p*-CH_3), 4.61 (s, 1H, Ge−H), 6.68 (d, 2H, *m*-C_6H_3), 6.82 (s, 4H, *m*-Mes), 6.97 (t, 1H, *p*-C_6H_3). $^{13}C\{^1H\}$ NMR (C_7D_8): δ 21.4 (*p*-CH_3), 21.8 (*o*-CH_3), 128.6, 129.1, 129.5, 136.1, 136.3, 136.4, 141.5, 148.9 (ArC). IR (Nujol): ν (Ge−H): 2113, 1731.

$Ar^#_2GeH(NH_2)$ (2). To a deep purple solution of $GeAr^#_2$[15] (0.20 g, 0.29 mmol) in toluene (50 mL), cooled to ca. −78 °C, were added several drops of liquid ammonia. The solution immediately became pale yellow and was stirred for a further 30 min. Warming slowly to room temperature afforded a colorless solution which was concentrated to 30 mL to give colorless crystals of **2**. Yield: 75%. Mp: 208 °C. ^1H NMR (C_7D_8): δ −0.37 (s, 2*H*, NH_2), 1.79 (s, 12H, *o*-CH_3), 1.93 (s, 12H, *o*-CH_3), 2.25 (s, 12H, *p*-CH_3), 5.47 (s, 1H, Ge−*H*), 6.68 (d, 4H, *m*-C_6H_3), 6.72 (s, 4H, *m*-Mes), 6.76 (s, 4H, *m*-Mes), 7.00 (t, 2H, *p*-C_6H_3).$^{13}C\{^1H\}$ δ 21.8 (*p*-CH_3), 22.8 (*o*-CH_3), 22.9 (*o*-CH_3), 149.3, 141.9, 140.1, 137.7, 137.5, 137.1, 131.2 (ArC), signal of *i*-C_6H_3 was not observed. IR (Nujol): υ (Ge−H): 2110 cm^{-1}; υ (NH_2, weak): 3397, 3323 cm^{-1}.

$Ar'_2GeH(NH_2)$ (3). A deep blue solution of $GeAr'_2$[16] (0.4 g, 0.46 mmol) in toluene (60 mL) was cooled to ca. −78 °C, and several drops of liquid ammonia were added. The solution immediately became pale yellow. Warming slowly to room temperature afforded a colorless solution which was concentrated to ca. 30 mL to give colorless crystals of **3**. Yield: 70%. Mp: 285 °C. ^1H NMR (C_6D_6) δ −0.37 (s, 2*H*, NH_2), 0.78 (d, 6H, $^3J_{HH}$ = 6.6 Hz, CH(CH_3)$_2$), 0.90 (d, 6H, $^3J_{HH}$ = 6.6 Hz, CH(CH_3)$_2$), 0.93 (d, 6H, $^3J_{HH}$ = 6.6 Hz, CH(CH_3)$_2$), 1.17 (d, 6H, $^3J_{HH}$ = 6.6 Hz, CH(CH_3)$_2$), 1.20 (d, 6H, $^3J_{HH}$ = 6.6 Hz, CH(CH_3)$_2$), 1.22 (d, 6H, $^3J_{HH}$ = 6.6 Hz, CH(CH_3)$_2$), 1.27 (d, 6H, $^3J_{HH}$ = 6.6 Hz, CH(CH_3)$_2$), 1.36 (d, 6H, $^3J_{HH}$ = 6.6 Hz, CH(CH_3)$_2$), 2.58 (septets, 2H, C*H*(CH$_3$)$_2$), 2.83 (septets, 2H, C*H*(CH$_3$)$_2$), 3.26 (septets, 2H, C*H*(CH$_3$)$_2$), 3.39 (septets, 2H, C*H*(CH$_3$)$_2$), 5.84 (s, 1H, *Ge*−*H*), 6.35(d, *m*-C_6H_3), 6.59 (d, *m*-C_6H_3), 6.71 (t, *p*-C_6H_3), 6.82 (t, *p*-C_6H_3), 6.87−7.37 (Dipp-H). $^{13}C\{^1H\}$ δ 23.9 (CH(CH$_3$)$_2$), 26.3 (CH(CH$_3$)$_2$), 30.7 (CH(CH$_3$)$_2$), 147.6, 146.5, 141.5, 139.3, 127.4, 127.0, 124.7, 124.4, 123.8 (ArC). IR (Nujol): υ (Ge−H): 2080 cm^{-1}; υ (NH_2, weak): 3383, 3313 cm^{-1}.

$Ar'GeH_3$ (4). A deep blue solution of $GeAr'_2$[16] (0.30 g, 0.35 mmol) in toluene (50 mL) was stirred at 65 °C for 2 h under a H_2 atmosphere to give a pale yellow solution. The solvent was removed under reduced pressure to afford a white powder which was characterized by ^1H NMR spectroscopy. ^1H NMR (C_6D_6): $Ar'GeH_3$: δ 1.08 (d, 12H, $^3J_{HH}$ = 6.6 Hz, CH(CH_3)$_2$), 1.25 (d, 12H, $^3J_{HH}$ = 6.6 Hz, CH(CH_3)$_2$), 2.82 (septets, 4H, C*H*(CH$_3$)$_2$), 3.58 (s, 3H, *Ge*−*H*), 6.89−7.31 (Ar−H). Ar′H: δ 1.11 (d, 12H, $^3J_{HH}$ = 6.6 Hz, CH(CH_3)$_2$), 1.14 (d, 12H, $^3J_{HH}$ = 6.6 Hz, CH(CH_3)$_2$), 2.90 (septets, 4H, C*H*(CH$_3$)$_2$), 6.89 (s, *1*-C_6H_4), 7.09 (d, 2H, *3*-C_6H_4), 7.10 (d, 4H, $^3J_{HH}$ = 6.6 Hz, *m*-C_6H_3-Pr$^i_2$)), 7.22 (t, 1H, $^3J_{HH}$ = 7.5 Hz, *4*-C_6H_4), 7.31 (t, 2H,$^3J_{HH}$ = 6.6 Hz, *p*-C_6H_3-Pr$^i_2$).

$[Ar^#Sn(\mu\text{-}NH_2)_2]_2$ (5). To a deep purple solution of $SnAr^#_2$[15] (0.2 g, 0.27 mmol) in toluene (40 mL), cooled to ca. −78 °C, were added several drops of liquid ammonia. The solution immediately became pale yellow and was stirred for a further 30 min. Warming slowly to room temperature afforded a pale yellow solution which was concentrated to 30 mL to give colorless crystals of **5**. Yield: 60%. Mp: 176 °C. ^1H NMR (C_7D_8): δ 0.93 (s, 2H, NH_2), 1.91 (s, 6H, *p*-CH_3), 1.97 (s, 12H, *o*-CH_3), 6.62 (s, 4H, *m*-Mes), 6.75 (d, 2H, *m*-C_6H_3), 7.08 (t, 1H, *p*-C_6H_3). $^{13}C\{^1H\}$ NMR(C_7D_8): δ 22.1 (*p*-CH_3), 21.8 (*o*-CH_3), 148.5, 142.7, 141.6, 140.2, 136.9, 136.8, 136.4(ArC), signal of *i*-C_6H_3 was not observed. $^{119}Sn\{^1H\}$: 313. IR (Nujol): υ (NH_2, weak): 3358, 3270 cm^{-1}.

$[Ar'Sn(\mu\text{-}H)]_2$ (6). A solution of $SnAr'_2$[16] (1.15 g, 1.26 mmol) in toluene (50 mL) was stirred at 65° for 2 h under a H_2 atmosphere to give a green solution. The mixture was concentrated to ca. 10 mL under vacuum which afforded orange crystals of **6** upon cooling to ca. −16°. Yield: 39%. ^1H NMR (C_6D_6): 0.93 (d, 6H, $^3J_{HH}$ = 6.6 Hz, CH(CH_3)$_2$, 1.02 (d, 6H, $^3J_{HH}$ = 6.6 Hz, CH(CH_3)$_2$), 1.04 (d,

(15) Simons, R. S.; Pu, L.; Olmstead, M. M.; Power, P. P. *Organometallics* **1997**, *16*, 1920.

(16) Spikes, G. H.; Peng, Y.; Fettinger, J. C.; Power, P. P. *Z. Anorg. Allg. Chem.* **2006**, *632*, 1005.

Table 1. Selected Crystallographic Data for Compounds **1**, **2**, **3**, **5**, and **8**

	1	2	3	5	8
formula	$C_{48}H_{52}Ge$	$C_{55}H_{61}GeN$	$C_{67}H_{85}GeN$	$C_{55}H_{62}N_2Sn_2$	$C_{88}H_{110}N_2Sn_2$
fw	701.51	808.66	976.97	988.45	1433.20
color, habit	colorless, needle	colorless, needle	colorless, needle	colorless, block	colorless, block
cryst syst	orthorhombic	monoclinic	monoclinic	triclinic	triclinic
space group	*Fdd*2	$P2_1/c$	$C2/c$	$P\bar{1}$	$P\bar{1}$
a, Å	20.701(5)	8.5642(10)	13.581(6)	8.6345(12)	12.0051(6)
b, Å	43.699(11)	21.275(3)	35.514(6)	12.8195(18)	13.3719(7)
c, Å	8.231(2)	23.860(3)	11.683(2)	21.717(3)	13.6933(7)
α, deg	90	90	90	102.6280(19)	110.5722(7)
β, deg	90	89.973(2)	90.550(3)	95.034(2)	102.3158(7)
γ, deg	90	90	90	93.0434(19)	103.5991(7)
V, Å^3	7445(3)	4347.4(10)	5556(2)	2330.1(6)	1891.60(17)
Z	8	4	4	2	1
cryst dim, mm^3	0.15 × 0.11 × 0.07	0.52 × 0.29 × 0.17	0.28 × 0.12 × 0.09	0.12 × 0.09 × 0.07	0.41 × 0.37 × 0.34
d_{cal}, g cm^{-3}	1.252	1.235	1.168	1.409	1.258
μ, mm^{-1}	0.846	0.743	0.592	1.110	0.705
no. of reflns	4309	9945	5503	10655	8667
no. of obsd reflns	3476	9369	3313	8798	7861
no. of param	226	540	334	584	425
R_1 obsd reflns	0.0534	0.0308	0.0746	0.0325	0.0220
wR_2, all	0.1520	0.0818	0.1381	0.0870	0.0578

Scheme 1. Summary of the Reactions of EAr_2 (E = Ge, Sn; Ar = Ar# (C_6H_3-2,6-(C_6H_2-2,4,6-Me_3)$_2$) or Ar′ (C_6H_3-2,6-(C_6H_3-2,6-^{i}Pr$_2$)$_2$)) with H_2 and NH_3

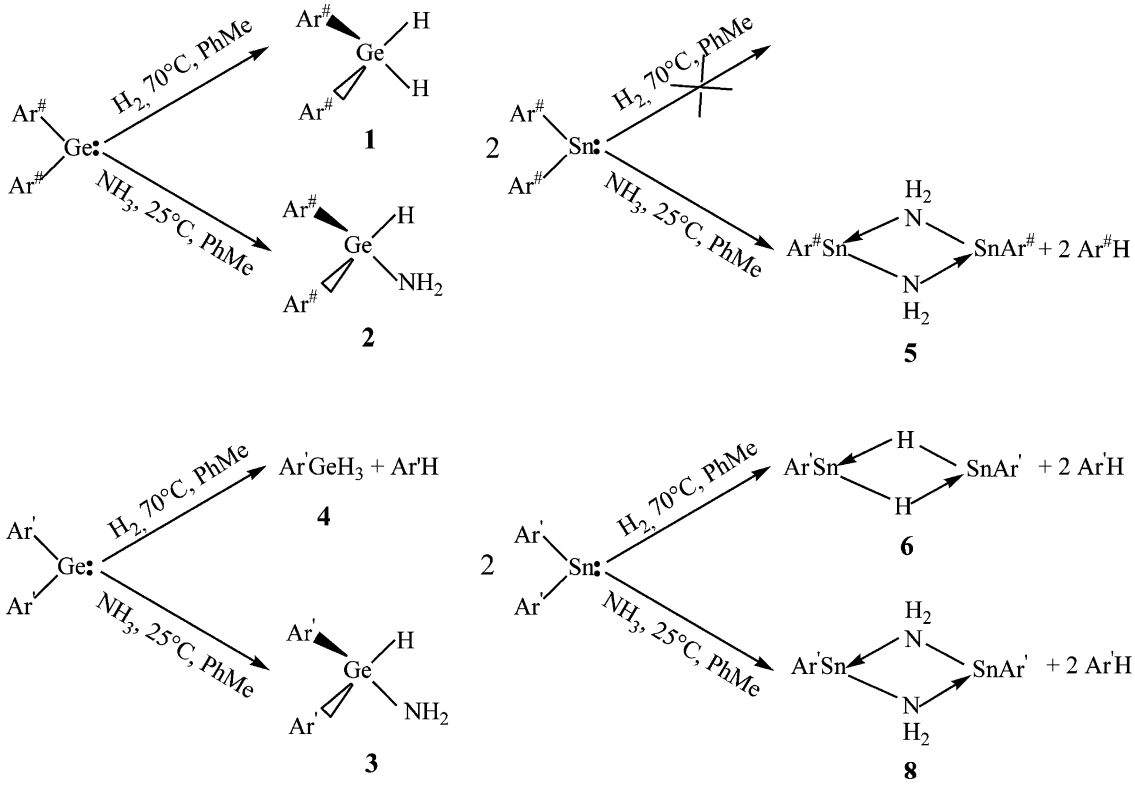

6H, $^3J_{HH}$ = 6.6 Hz, CH(CH_3)$_2$), 1.11 (d, 6H, $^3J_{HH}$ = 6.6 Hz, CH(CH_3)$_2$), 3.00 (overlap septets, 4H, CH(CH$_3$)$_2$), 7.03 (d, 4H,$^3J_{HH}$ = 7.5 Hz, m-*Dipp*), 7.10 (m, 3H, ArH), 7.30 (t, 2H, $^3J_{HH}$ = 7.5 Hz, *p*-C_6H_2-Pr$^i_2$), 9.13 (s, 1H, $^1J_{Sn-H}$ = ca. 89 Hz, Sn-*H*). ^{119}Sn{^{1}H} NMR: δ 657.

[Ar′Sn(*μ*-D)]$_2$ (7). A solution of SnAr′$_2$[16] (1.05 g, 1.15 mmol) in toluene (50 mL) was stirred at 65° for 2 h under a D_2 atmosphere to give a dark green solution. The mixture was concentrated to ca. 10 mL under vacuum which afforded orange crystals of **7** upon cooling to ca. −16°. Yield: 45%. ^{1}H NMR (C_6D_6): 0.93 (d, 6H, $^3J_{HH}$ = 6.6 Hz, CH(CH_3)$_2$, 1.02 (d, 6H, $^3J_{HH}$ = 6.6 Hz, CH(CH_3)$_2$), 1.04 (d, 6H, $^3J_{HH}$ = 6.6 Hz, CH(CH_3)$_2$), 1.11 (d, 6H, $^3J_{HH}$ = 6.6 Hz, CH(CH_3)$_2$), 3.00 (overlap septets, 4H, CH(CH$_3$)$_2$), 7.03 (d, 4H,$^3J_{HH}$ = 7.5 Hz, m-*Dipp*), 7.10−7.28 (m, ArH). ^{2}H NMR (C_7H_8): 8.98 (s). ^{119}Sn{^{1}H} NMR (C_7D_8): δ 610 (br).

[Ar′Sn(*μ*-NH$_2$)]$_2$ (8). To a deep blue solution of SnAr′$_2$[16] (0.45 g, 0.5 mmol) in toluene (50 mL) at −78° was added several drops of liquid ammonia. The solution became light yellow. Warming to room temperature produced a colorless solution, which was concentrated to ca. 30 mL under reduced pressure to give colorless crystals that were identified as **8** on the basis of NMR spectroscopy and X-ray crystallography. Yield: 55%. Mp: 120−125°. ^{1}H NMR (C_7D_8): δ 0.72 (s, 2H, NH_2), 1.48 (d, 12H, $^3J_{HH}$ = 6.6 Hz, CH(CH_3)$_2$), 1.63 (d, 12H, $^3J_{HH}$ = 6.6 Hz, CH(CH_3)$_2$), 3.42 (septets, 4H, CH(CH$_3$)$_2$), 7.48(t, 2H, *p*-Dipp), 7.58 (t, 1H, $^3J_{HH}$ = 6.6 Hz, *p*-C_6H_3), 7.65 (d, 4H,$^3J_{HH}$ = 6.6 Hz, *m*-C_6H_2-Pr$^i_2$)), 7.68 (d, 2H,

Table 2. Selected Bond Lengths (Å) and Angles (deg) for **1**, **2**, **3**, **4**, **5**, **6**, and **8** and for EAr_2 (E = Ge or Sn; Ar = Ar# or Ar′)

	$GeAr^{\#}_2$ [15]	$GeAr'_2$ [16]	**1**	**2**	**3**	**4**
Ge−C (Å)	2.033(4)	2.04(1)	1.973(3)	1.997(1)	1.992(4)	1.979(2)
C−Ge−C (deg)	114.4(2)	112.77(9)	127.9(2)	120.41(7)	—	—
Ge−H (Å)	—	—	1.30(4)	1.45(3)	1.56(2)	1.445(10)
H−Ge−H/N (deg)	—	—	101(2)	104.9(11)	106(4)	—
Ge−N (Å)	—	—	—	1.852(2)	—	—

	$SnAr^{\#}_2$ [15]	$SnAr'_2$ [16]	**5**	**6**	**8**
Sn−C (Å)	2.225(5)	2.255(2)	2.235(3)	2.221(6)	2.238(2)
C−Sn−C (deg)	114.7(2)	117.56(8)	—	—	—
Sn−H (Å)	—	—	—	1.91(8)	—
Sn−N (Å)	—	—	2.218(2)	—	2.192(2)

$^3J_{HH}$ = 6.6 Hz, m-C_6H_3). $^{13}C\{^1H\}$ NMR(C_7D_8): 24.3 ($CH(CH_3)_2$), 26.6 ($CH(CH_3)_2$), 31.22 ($CH(CH_3)_2$), 126.5, 128.9, 129.5, 130.2, 147.2, 157.4(Ar−C), signal of *i*-C_6H_3 was not observed. $^{119}Sn\{^1H\}$ NMR (C_7D_8): δ 280. IR (Nujol): υ 3357, 3260 cm^{-1}(υ NH_2, weak).

Computational Methods. All the calculations were carried out with the density functional theory (DFT) in the Gaussian 03 program.[17] The geometry optimization was performed at B3PW91 level by using a double-ζ basis set (Lanl2dz) plus a d-type polarization function (d exponent 0.246 for Ge or 0.183 for Sn) along with the effective core potential (Lanl2 ECP)[18] for Ge or Sn atoms, and the 3-21G basis set for all other atoms. To improve energies, single point calculations were done with the larger basis set [433111/43111/4] plus two d polarization functions (d exponents 0.382 and 0.108) for Ge or [4333111/433111/43] plus two d polarization functions (d exponents 0.253 and 0.078) for Sn[19] and the basis set 6-31G(d, p) for all other atoms. To explore the possible solvent effects on the reactions, polarized continuum model (PCM)[20] calculations, based on the gas-phase optimized structures, were performed for toluene (ε = 2.379) at 298.15K. Zero-point vibrational energy corrections were also included. In order to obtain more accurate HOMO−LUMO and singlet−triplet gaps for EAr_2 (*E* = Ge or Sn; Ar = $Ar^{\#}$ or Ar′), geometries of these four molecules were fully optimized at B3PW91 level with the larger basis sets described in the above computational methods. All the transition structures (TS) were located on the potential energy surfaces and verified by one imaginary frequency. The intrinsic reaction coordinates (IRC) calculations confirmed the connectivity of TS with reactants and products.

X-ray Crystallographic Studies. Crystals of **1**, **2**, **3**, **5**, and **8** were removed from a Schlenk tube under a stream of nitrogen and immediately covered with a thin layer of hydrocarbon oil. A suitable crystal was selected, attached to a glass fiber on a copper pin, and quickly placed in a N_2 cold stream on the diffractometer.[21] Data were collected at 90 K (**1**, **2**, **5**) on a Bruker APEX instrument with use of Mo Kα (λ = 0.710 73 Å) radiation and a CCD area detector. Data for **3** and **8** were collected at 90 K on a Bruker SMART 1000 diffractometer with use of Mo Kα (λ = 0.710 73 Å) radiation and a CCD area detector. For compounds **1** and **8**, the SHELX version 6.1 program package was used for the structure solutions and refinements. Absorption corrections were applied using the SADABS program.[22] Crystals of **2**, **3**, and **5** were determined to be twinned, and an alternative procedure (see Supporting Information) was used to "de-twin" the data and afford a solution. The crystal structures were solved by direct methods and refined by full-matrix least-squares procedures. All non-H atoms were refined anisotropically. All carbon-bound H atoms were included in the refinement at calculated positions using a riding model included in the SHELXTL program. Some details of the data collection and refinement are given in Table 1.

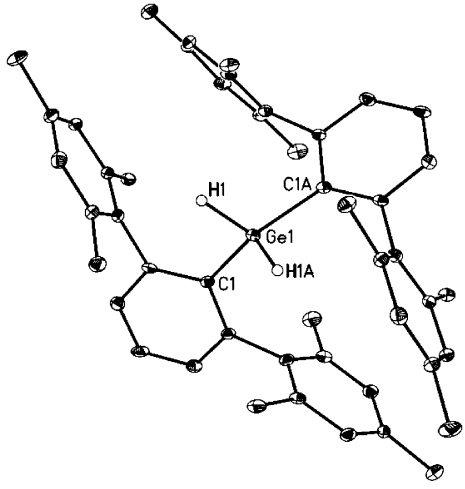

Figure 1. Thermal ellipsoid (30%) drawing of **1**. Hydrogen atoms except those on germanium are not shown. Selected bond length (Å) and angles (deg): Ge1−C1 1.973(3), Ge1−H1 1.30(4), C1−Ge1−C1A 127.9 (2).

Result and Discussion

Synthesis and Spectroscopy. The synthetic work reported in this paper is summarized in Scheme 1. Compounds **6**, **7**, and **8** were reported in a preliminary communication.[5]

Compound **1** was obtained by treatment of a dark purple solution of $GeAr^{\#}_2$[15] with H_2 at 60−70 °C. The solution faded to a pale purple color within 3−4 h, from which colorless, needle-like crystals of $Ar^{\#}_2GeH_2$ (**1**) could be obtained upon concentration and cooling to ca. −16 °C. The ^1H NMR spectrum displayed a Ge−H signal at 4.61 ppm with the correct intensity ratio with respect to the aryl ligand resonances. The FT- IR spectrum of **1** displayed two strong bands at 2113 and 1731 cm^{-1} which were assigned to the symmetric and antisymmetric Ge−H stretching modes. The compound **1** is thermally stable and melts near 265 °C without decomposition.

The reaction of $GeAr^{\#}_2$[15] with excess NH_3 in toluene rapidly discharged the color. Concentration of the solution gave colorless crystals of $Ar^{\#}_2Ge(H)NH_2$ (**2**). The FT-IR spectrum displayed two weak but sharp bands at 3397 and 3323 cm^{-1} that are due to the N−H stretching modes of the

(17) Frisch, M. J. *Gaussian 03*, revision E.01; Gaussian, Inc.: Wallingford, CT, 2004.
(18) Wadt, W. R.; Hay, P. J. *J. Chem. Phys.* **1985**, *82*, 284.
(19) (a) *Gaussian Basis Sets for Molecular Calculations*; Elsevier: Amsterdam, 1984. (b) Takagi, N.; Nagase, S. *Organometallics* **2007**, *26*, 469.
(20) (a) Miertus, S.; Scrocco, E.; Tomasi, J. *Chem. Phys.* **1981**, *55*, 117. (b) Tomasi, J.; Mennucci, B.; Cammi, R. *Chem. Rev.* **2005**, *105*, 2999.
(21) Hope, H. *Prog. Inorg. Chem.* **1995**, *41*, 1.
(22) *SADABS*, An empirical absorption correction program, part of the SAINTPlus NT version 5.0 package; Bruker AXS: Madison, WI, 1998.

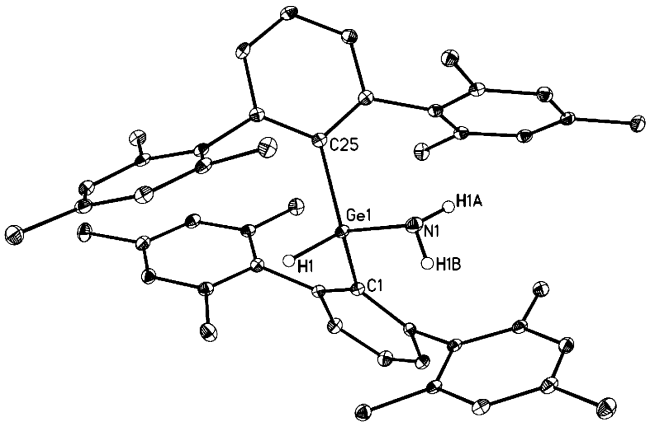

Figure 2. Thermal ellipsoid (30%) drawing of **2**. Hydrogen atoms except those on germanium and nitrogen are not shown. Selected bond length (Å) and angles (deg): Ge1−C1 2.0079(18), Ge1−C25 1.9869(18), Ge1−H1 1.45(3), Ge1−N1 1.8517(18), N1−H1A 0.92(4), N1−H1B 0.85(3), C1−Ge1−C25 120.41(7), H1−Ge1−N1 104.92(11), Ge1−N1−H1A 108(2), Ge1−N1−H1B 112(2), H1A−N1−H1B 108(3).

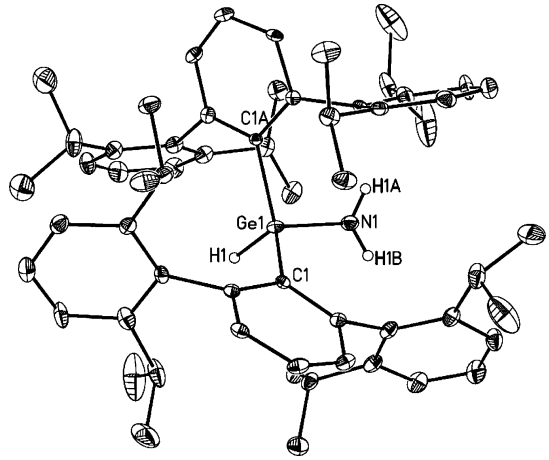

Figure 3. Thermal ellipsoid (30%) drawing of **3**. Hydrogen atoms except those on germanium and nitrogen are not shown. Selected bond length (Å) and angles (deg): Ge1−C1 1.992(4), Ge−N1 1.883(7), Ge1−H1 1.56(7), N1−H1A 0.88(2), N1−H1B 0.88(2), C1−Ge1−C1A 119.9(2), C1−Ge1−H1 113(4), C1A−Ge1−H1 108(4), C1−Ge1−N1 101.5(3), C1A−Ge1−N1 108.0(3).

amide group and one band at 2110 cm^{-1} assignable to the terminal Ge−H stretching mode. The ^1H NMR spectrum of **2** in C_7D_8 also confirmed the presence of NH_2 and Ge−H moieties via signals at −0.37 and 5.47 ppm respectively, in the correct intensity ratio to each other and to the aryl ligand resonances. In a similar way $GeAr'_2$[16] gave colorless crystals of $Ar'_2GeH(NH_2)$ (**3**) upon treatment with NH_3. The FT-IR spectrum displayed two weak but sharp bands at 3383 and 3313 cm^{-1} and one band at 2080 cm^{-1} assignable to the NH_2 and Ge−H stretching modes. The ^1H NMR spectrum of **3** in C_7D_8 also confirmed the presence of NH_2 and Ge−H moieties via signals at −0.37 and 5.84 ppm respectively, in the correct intensity ratio to each other and to the aryl ligand resonances. In contrast to the reaction with NH_3, treatment of $GeAr'_2$[16] with excess H_2 affords a solution containing $Ar'GeH_3$ (**4**) and Ar′H. Probably, the H_2 adds to $GeAr'_2$ which decomposes to Ar′GeH and Ar′H (detected by ^1H NMR). The Ar′GeH, which is apparently in equilibrium with its Ge−Ge bonded

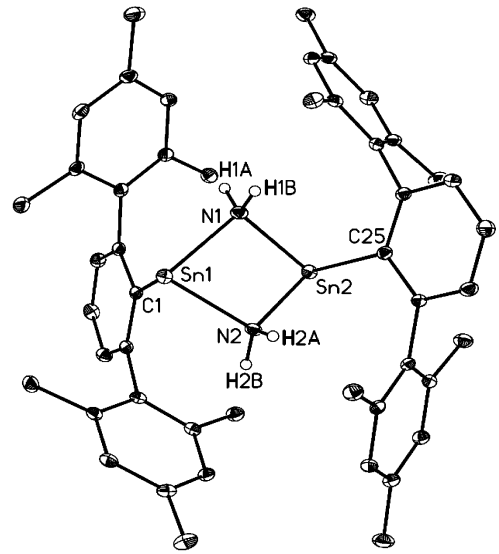

Figure 4. Thermal ellipsoid (30%) drawing of **5**. Hydrogen atoms except those on nitrogen are not shown. Selected bond length (Å) and angles (deg): Sn1−C1 2.240(3), Sn2−C25 2.230(3), Sn1−N1 2.222(2), Sn1−N2 2.223(2), Sn2−N1 2.214(2), Sn2−N2 2.212(2), N1−H1A 0.92(2), N1−H1B 0.92(2), C1−Sn1−N1 95.03(8), N1−Sn1−N2 75.49(7), C1−Sn1−N2 96.10(8), Sn1−N1−Sn2 100.51(8), Sn1−N2−Sn2 100.56(8), C25−Sn2−N2 93.99(8), N1−Sn2−N2 75.87(8).

Table 3. Selected Calculated Bond Lengths (Å) and Angles (deg) for **1**, **2**, **5**, and **6** and for EAr_2 (E = Ge or Sn; Ar = $Ar^{\#}$ or Ar′)

	$GeAr^{\#}_2$	$GeAr'_2$	**1**	**2**
Ge−C (Å)	2.076(av)	2.091(av)	2.008(av)	2.017(av)
C−Ge−C (deg)	116.4	111.9	132.5	121.5
Ge−H (Å)	—	—	1.545(av)	1.547
H−Ge−H/N (deg)	—	—	108.4	106.4
Ge−N (Å)	—	—	—	1.843

	$SnAr^{\#}_2$	$SnAr'_2$	**5**	**6**
Sn−C (Å)	2.282(av)	2.299(av)	2.261(av)	2.236
C−Sn−C (deg)	115.0	117.4	—	—
Sn−H (Å)	—	—	—	1.977(av)
Sn−N (Å)	—	—	2.198(av)	—

Table 4. Calculated HOMO−LUMO and Singlet−Triplet State Energy (S−T) Differences for EAr_2 (E = Ge or Sn, Ar = $Ar^{\#}$ or Ar) in kcal mol^{-1}

	λ_{max} nm (kcal mol^{-1})	calcd λ_{max} nm (kcal mol^{-1})	$\Delta E_{(HOMO-LUMO)}$	$\Delta E_{(S-T)}$
$GeAr^{\#}_2$	578 (49.5)	526 (54.4)	66.62	15.9
$GeAr'_2$	608 (47.1)	598 (47.8)	63.63	17.4
$SnAr^{\#}_2$	553 (51.8)	473 (60.5)	64.55	17.8
$SnAr'_2$	600 (47.7)	542 (52.8)	61.57	18.7

dimer,[23] may then undergo addition of H_2 to form $Ar'GeH_3$. The ^1H NMR spectrum of the reaction mixture displayed a signal at 3.58 ppm due to the Ge−H hydrogens in $Ar'GeH_3$[1] and two doublets at 1.11 and 1.14 ppm specifically for the $-CH(CH_3)_2$ group in Ar′H.[5]

The addition of excess ammonia to a dark purple solution of $SnAr^{\#}_2$[15] in toluene produced a colorless solution from which colorless crystals of $\{Ar^{\#}Sn(\mu\text{-}NH_2)\}_2$ (**5**) were isolated in good yield. The N−H stretching bands of **5** (3358 and

(23) Richards, A. F.; Phillips, A. D.; Olmstead, M. M.; Power, P. P. *J. Am. Chem. Soc.* **2003**, *125*, 3204.

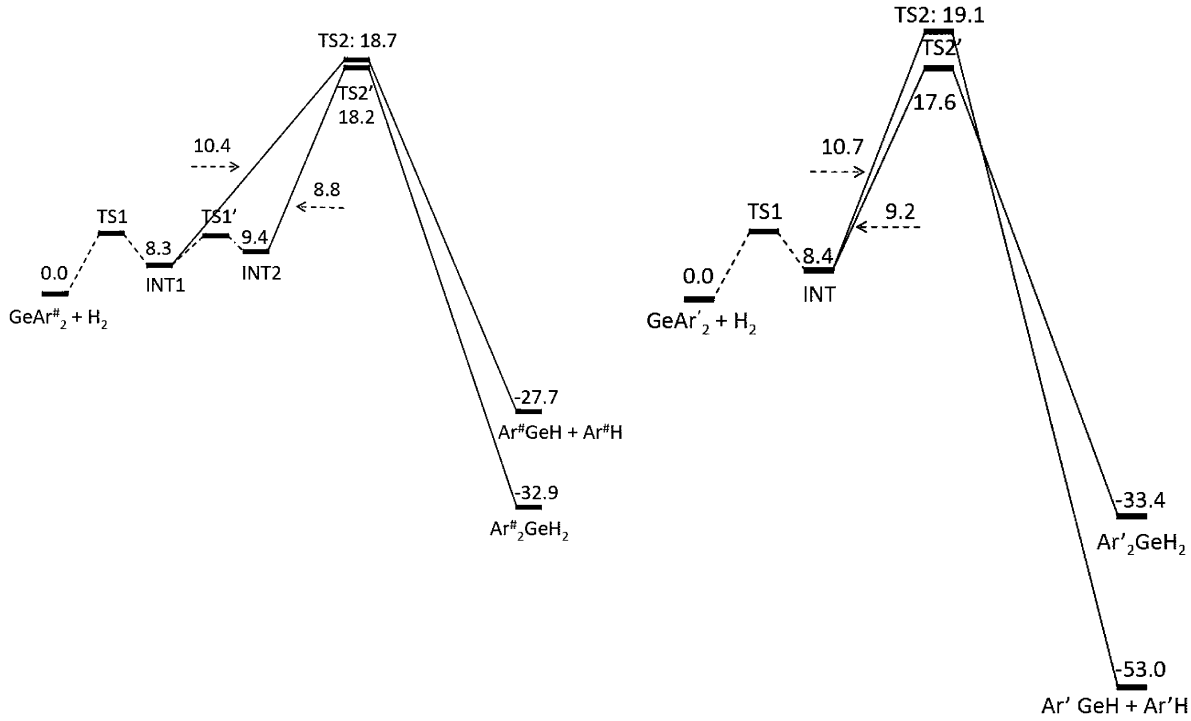

Figure 5. Calculated relative energies (kcal mol^{-1}) for the reaction of $GeAr_2$ (Ar = Ar# or Ar′) with H_2 at the B3PW91 level.

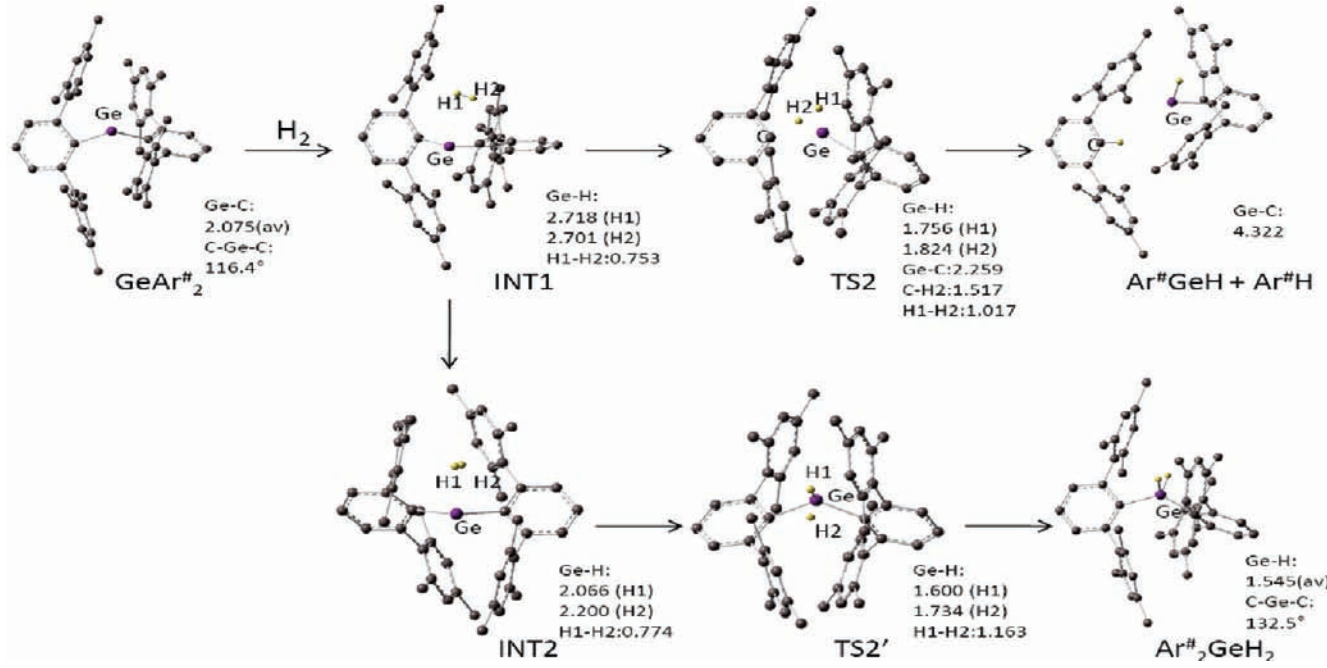

Figure 6. Drawings of the intermediates and transition states with selected distances (Å) and angles (deg) for the reaction of $GeAr^{\#}_2$ with H_2. H atoms (except Ge−H) are not shown.

3270 cm^{-1}) are close to those of $\{Ar'Sn(\mu\text{-}NH_2)_2\}_2$ (**8**) (3357, 3260 cm^{-1})[5] and of $\{Ar^*Sn(\mu\text{-}NH_2)_2\}_2$ (Ar* = C_6H_3-2,6-(C_6H_2-2,4,6-$^i Pr_3$)$_2$) (3370, 3290 cm^{-1})[24] which was synthesized independently by the direct reaction of Ar*SnCl with NH_3. The ^{119}Sn NMR spectrum afforded a singlet at 313 ppm which is close to the 280 ppm observed in **8**[5] and 286 ppm in $\{Ar^*Sn(\mu\text{-}NH_2)_2\}_2$.[24]

(24) Stanciu, C.; Hino, S. S.; Stender, M.; Richards, A. F.; Olmstead, M. M.; Power, P. P. *Inorg. Chem.* **2005**, *44*, 2774.

Treatment of a solution of $SnAr^{\#}_2$ with H_2 under the identical conditions to those employed for $GeAr^{\#}_2$ for periods as long as two months afforded no reaction. This was unexpected in view of the less crowded tin environment. However the energy gap corresponding to the n→p transition at 553 nm in $SnAr^{\#}_2$[15] is about 4 kcal mol^{-1} higher than that of $SnAr'_2$[16] which may explain its diminished reactivity (see Table 4 for computed λ_{max} and HOMO−LUMO energy differences which also indicate increased values for $SnAr^{\#}_2$ vs $SnAr'_2$). The bulkier $SnAr'_2$[16] reacts in solution with H_2

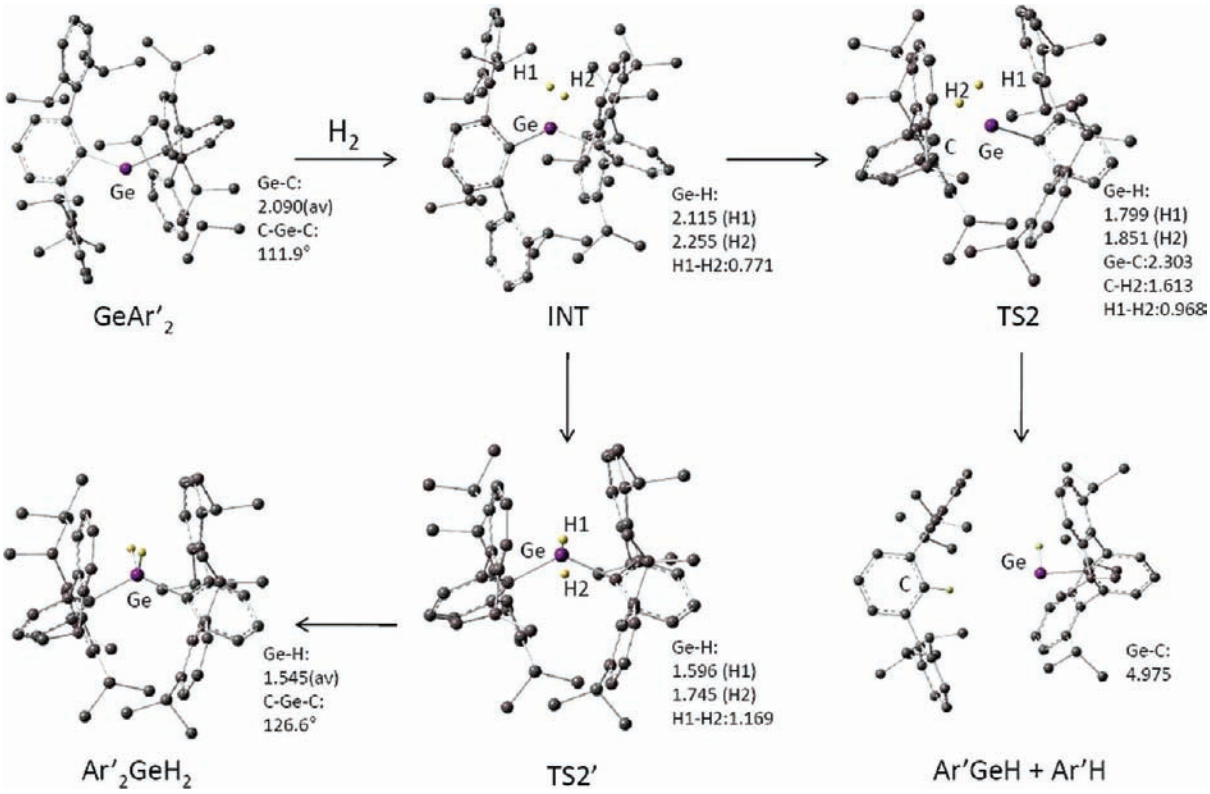

Figure 7. Drawings of the intermediates and transition states with selected distances (Å) and angles (deg) for the reaction of $GeAr'_2$ with H_2. H atoms (except Ge−H) are not shown.

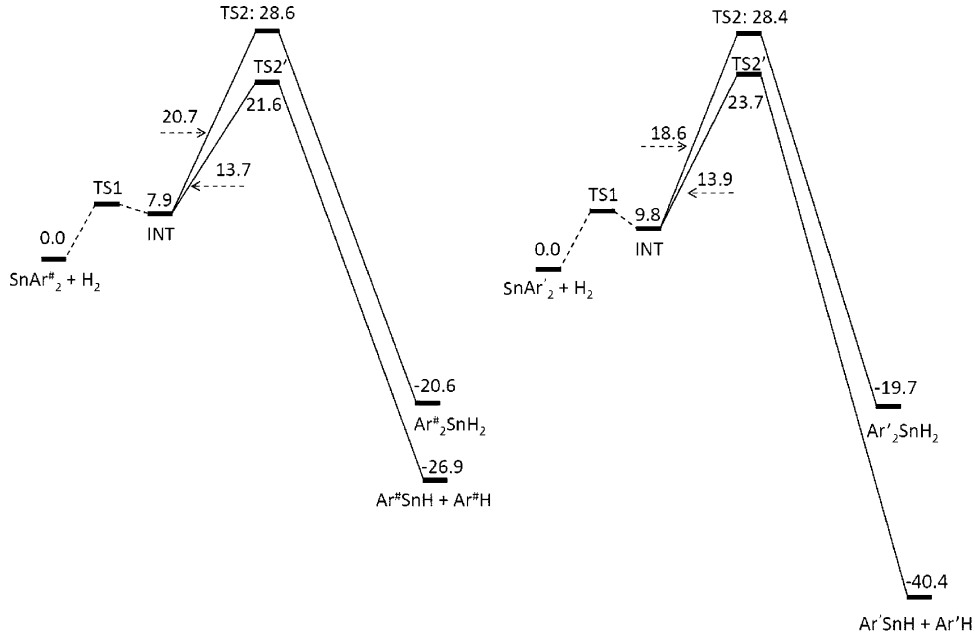

Figure 8. Calculated relative energies (kcal mol^{-1}) for the reaction of $SnAr_2$ (Ar = Ar# or Ar′) with H_2 at the B3PW91 level.

or D_2 gas at 60−70° within 1 h to afford a color change to dark green from which orange crystals of **6** or **7** could be obtained. Examination of the ^1H and ^2H NMR spectrum confirmed the formation of bridging Sn(II) hydride.[5]

From the perspective of bond enthalpies, the addition of H_2 or NH_3 to the germanium and tin diaryls is favored because of the relatively high Ge−H, Sn−H, Ge−N and Sn−N bond strengths, which have the approximate values of 74,[25] 62,[25] 70[26] and 60[26] kcal mol^{-1} respectively and are sufficiently large to compensate for cleavage of the H−H or N−H bonds (ca. 103 or 95 kcal mol^{-1} respectively). The elimination of the arene Ar#H or Ar′H (C−H = ca. 90−95 kcal mol^{-1})[27] from the tetravalent addition products with concomitant cleavage of an M-C (Ge−C = ca. 73, Sn−C = ca. 61 kcal mol^{-1})[25] and an M-H bond is seemingly unfavorable enthalpically for both tin and germanium. However it is ca. 25 kcal mol^{-1} less unfavorable for tin. This, combined with the greater lone pair stability,[28] is apparently

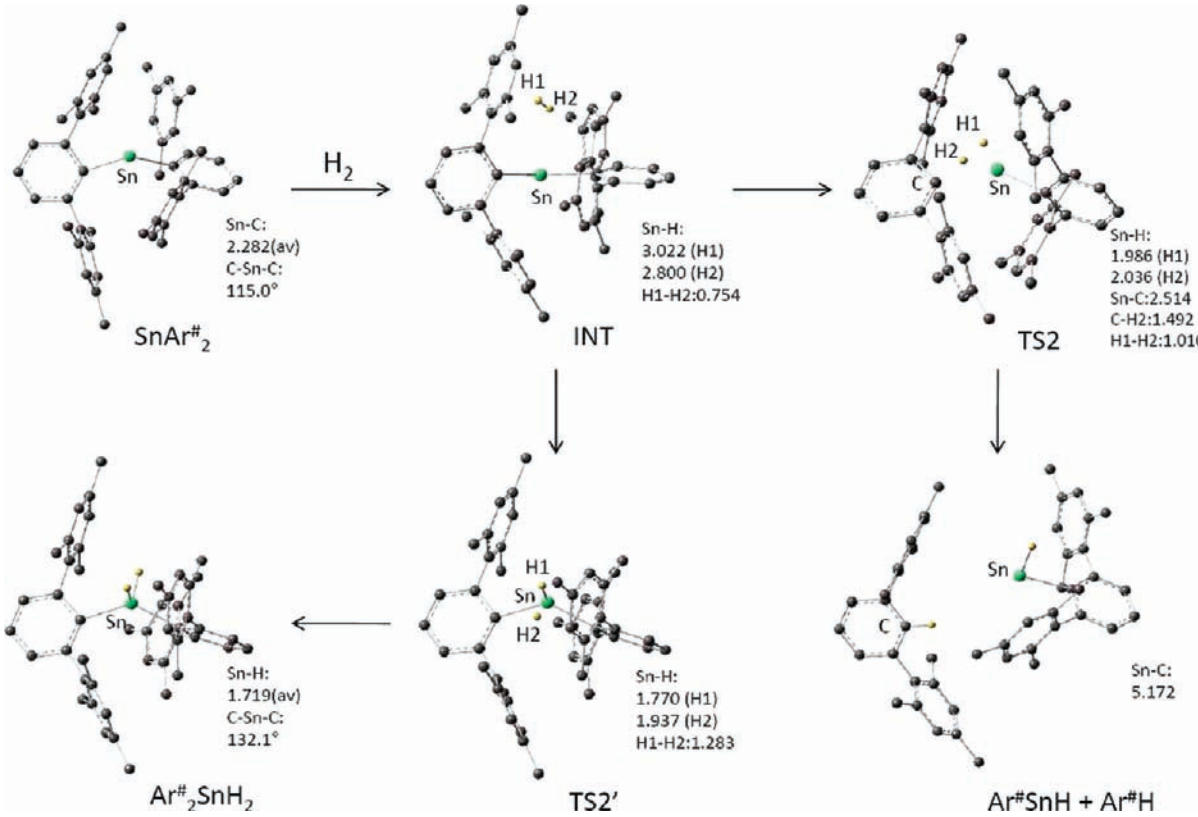

Figure 9. Drawings of the intermediates and transition states with selected distances (Å) and angles (deg) for the reaction of $SnAr^{\#}_2$ with H_2. H atoms (except Sn−H) are not shown.

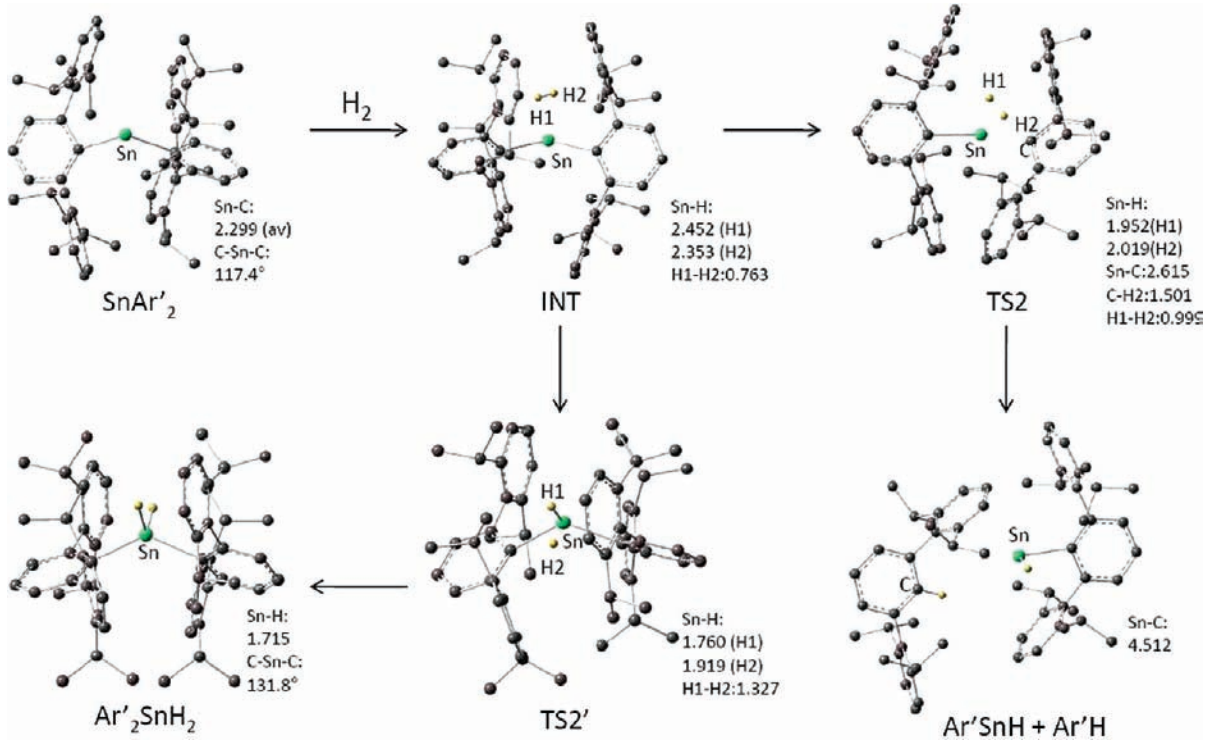

Figure 10. Drawings of the intermediates and transition states with selected distances (Å) and angles (deg) for the reaction of $SnAr'_2$ with H_2. H atoms (except Sn−H) are not shown.

sufficient to favor elimination for the tin compounds. It should be borne in mind that these arguments do not take into account other factors such as entropy or the dimeric structures of the eliminated product hydrides or amides.

X-ray Crystal Structures. Selected structural data for **1**, **2**, **3**, **5**, and **8** and their diaryl precursors are given in Table 2. The X-ray crystal structure of **1** showed that the molecule possessed a crystallographic 2-fold axis of symmetry and that the

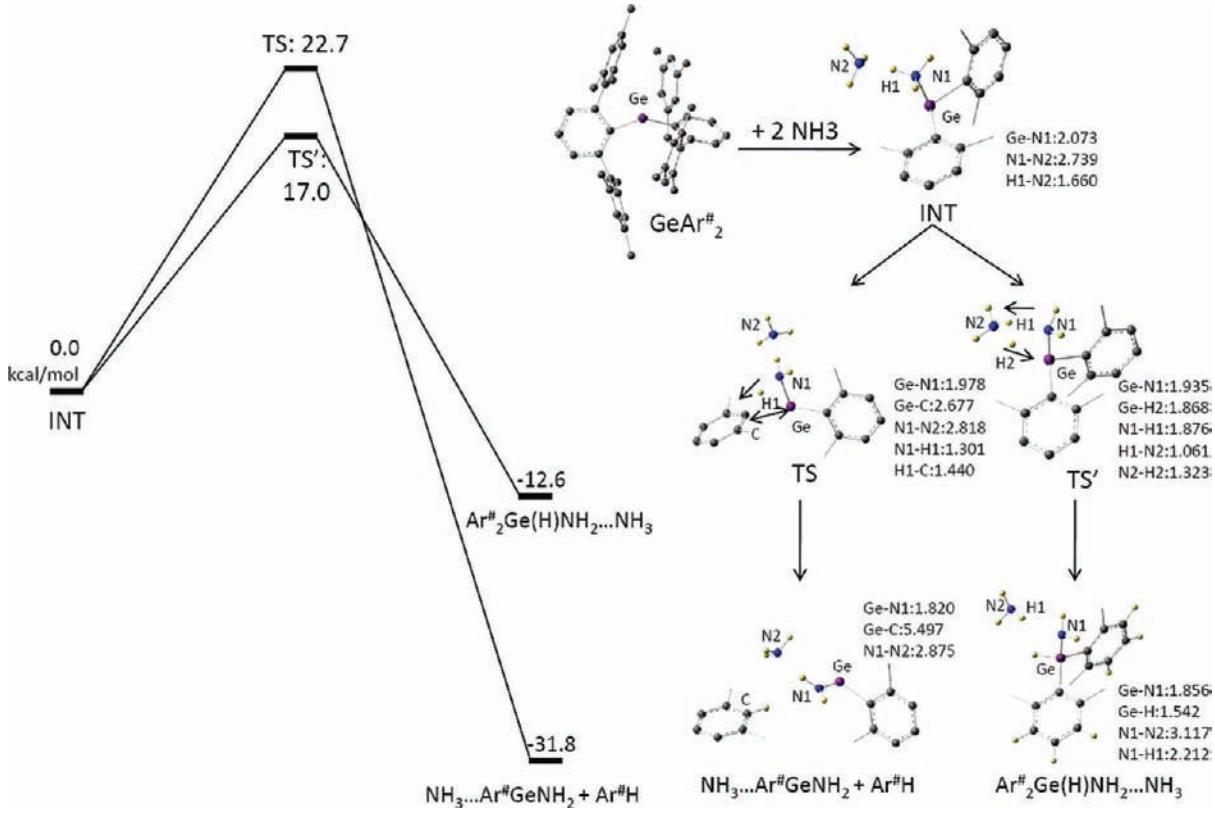

Figure 11. Calculated energy and drawings of intermediates and transition states with selected distances (Å) and angles (deg) for the reaction of $GeAr^{\#}_2$ with NH_3 at the B3PW91 level.

germanium had a distorted tetrahedral coordination in which both $Ar^{\#}$ ligands and the added hydrogen are bound to germanium. There is a wide angle of 127.9(2)° between the $Ar^{\#}$ substituents. The terminal Ge−H distance is 1.30(4) Å, which is shorter than the Ge−H distance of 1.445(10) Å observed in $Ar'GeH_3$[1] or ca. 1.44(4) Å in the divalent germanium hydrides stabilized by bulkier aryl ligands Figure 1.[23]

The structure of **2** confirmed that the germanium had inserted into the N−H bond to afford the amido germanium hydride product with distorted tetrahedral coordination. The angle between the two $Ar^{\#}$ groups (120.41(7)°) was ca. 8° narrower than that observed in **1**. The Ge−N distance of 1.852(2) Å is similar to the 1.836 Å found in $N(GeH_3)_3$ [29] or the 1.876(5) Å in the divalent $Ge\{N(SiMe_3)_2\}_2$.[30] The Ge−H distance is 1.45(3) Å and is essentially the same as the Ge−H distance 1.445(10) Å in $Ar'GeH_3$.[1] Interestingly, the nitrogen displays a distorted trigonal pyramidal geometry with the sum of the angles at nitrogen of 324.72(2)° (Figure 2).

The structure of **3** is similar to that of **2** in which the germanium had inserted into the N−H bond to afford a Ge(IV) product with distorted tetrahedral coordination. The Ge−C distances are 1.992(4) Å and the angle between the Ar′ ligands is 119.9(2)° which is similar to that in **2**. The Ge−N distance is 1.883(7) Å and the Ge−H distance is 1.56(2) Å which is longer than that in **2** presumably as a result of the larger Ar′ substituents (Figure 3).

X-ray crystallographic data for **5** showed that the tin centers were bridged by two NH_2 groups to give a planar Sn_2N_2 core. Sn−N bridging distances (2.222(2) and 2.213(2) Å) are similar to those reported for $\{Ar'Sn(\mu\text{-}NH_2)\}_2$ (avg. 2.19 Å)[5] and $\{Ar^*Sn(\mu\text{-}NH_2)\}_2$ (Sn-*N* = 2.21 Å, Ar* = C_6H_3-2,6-(C_6H_2-2,4,6-Pr^i_3)$_2$).[24] The tins have terminally bound $Ar^{\#}$ ligands to yield strongly pyramidal coordination as shown by the sum of the angles at tin of 266.62(9)° Figure 4.

X-ray crystallographic examination of **6** showed that it had a very similar Sn(II) bridging hydride structure to those recently reported for Sn(II) hydride.[31] X-ray crystallography of **8** afforded a Sn(II) dimeric structure[5] in which the tin centers were symmetrically bridged by the NH_2 ligands.

Computational Data. DFT calculations revealed that the reactions of H_2 with EAr_2 (*E* = Ge or Sn; Ar = $Ar^{\#}$ or Ar′) occur by a broadly similar mechanism to that described for the stable carbene (Bu^t)(Pr^i_2N)C: by Bertrand and Schoeller[3] although the relative degrees of electron donation or acceptance by the frontier orbitals of the divalent group 14 molecules presumably differs. Selected calculated structural data are shown

(25) Aylett, B. J. *Organometallic Compounds*, Vol. 1, Part 2, 4th ed.; Chapman and Hall: London, 1997; p 2.
(26) Lappert, M. F.; Power, P. P.; Sanger, A. R.; Srivastava, R.; *Metal and Metalloid Amides*; Ellis Horwood-Willey: Chichester, 1980; p 17.
(27) Smith, M. B.; March, J. *March's Advanced Organic Chemistry*, 5th ed.; Wiley: New York, 2001; p 24.
(28) As the atomic number increases, the p-block elements display a preference for an oxidation state that is two less than the total number of available valence electrons thereby giving the appearance of increasing stability of the s-electrons (also known as the inert pair effect). This is the result of several factors which are discussed in Kutzelnigg, W. *Angew. Chem. Int. Ed.,* **1984**, *23*, 272. See also: Hall, M. B. *Inorg. Chem.* **1978**, *17*, 2261.
(29) Robiette, A. G.; Glidewell, C.; Rankin, D. W. H. *J. Chem. Soc. A* **1970**, *18*, 2835.
(30) Chorley, R. W.; Hitchcock, P. B.; Lappert, M. F.; Leung, W. P.; Power, P. P.; Olmstead, M. M. *Inorg. Chim. Acta* **1992**, *201*, 121.
(31) Rivard, E.; Fischer, R. C.; Wolf, R.; Peng, Y.; Merrill, W. A.; Schley, N. D.; Zhu, Z.; Pu, L.; Fettinger, J. C.; Teat, S. J.; Nowik, I.; Herber, R. H.; Takagi, N.; Nagase, S.; Power, P. P. *J. Am. Chem. Soc.* **2007**, *29*, 16197.

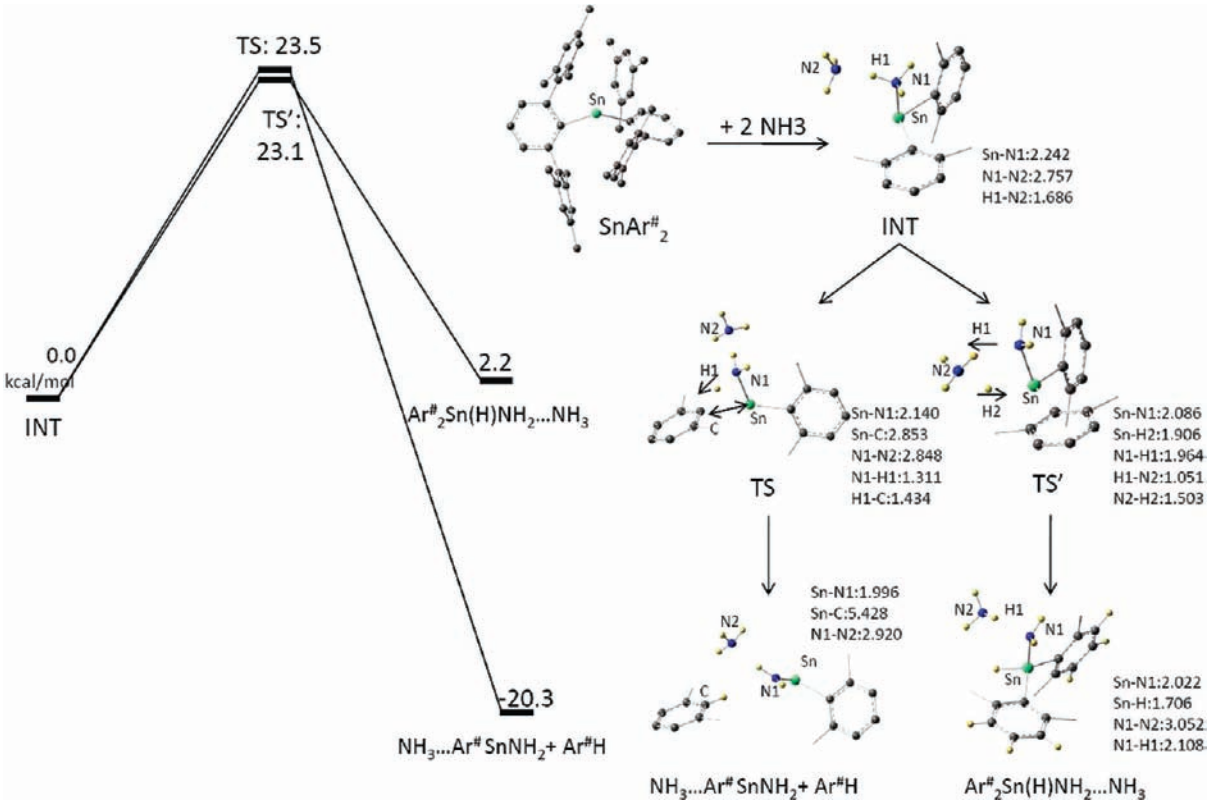

Figure 12. Calculated energy and drawings of intermediates and transition states with selected distances (Å) and angles (deg) for the reaction of $SnAr^{\#}_2$ with NH_3 at the B3PW91 level.

in Table 3. A comparsion of these data with the experimental results in Table 2 indicates close agreement. Calculated HOMO−LUMO and singlet−triplet (S-T) energy differences are provided in Table 4. The calculated absorption maxima for the electronic spectra are in good agreement with the experimental results. However the calculated HOMO−LUMO gaps are significantly higher, which can be attributed to steric strain in the ground state of the molecules.

Calculated reaction pathways for the reactions of $GeAr^{\#}_2$ and $GeAr'_2$ with H_2 are illustrated in Figure 5. Drawings of the intermediates and transition state structures are provided in Figures 6 and 7. For $GeAr^{\#}_2$ there is an initial formation of an intermediate (INT1, ie, intermediate 1) incorporating a weakly bound H_2 molecule in which the H atoms are almost equidistant (2.701 and 2.718 Å) from germanium and the H−H bond length (0.753 Å) remains close to that in the H_2 molecule.[32] This intermediate indicates that the initial interaction involves the σ-bond of the H_2 molecule with the empty 4p-orbital at the germanium atom. INT1 can transform via TS1′ (ie, transition state 1′) to INT2 which is slightly more stable than INT1 and has a similar H−H distance but much shorter and somewhat inequivalent (2.066 and 2.200 Å) Ge−H approaches. This may then transform via TS2′, which displays a considerable H−H elongation (1.163 Å) and short Ge−H distances, into the energetically favored $Ar^{\#}_2GeH_2$ product. The alternative pathway via TS2 to yield the Ge(II) product $Ar^{\#}GeH$, together with $Ar^{\#}H$ elimination, involves a higher energy route possibly because of the strength of the Ge−H and Ge−C bonds.[25] These theoretical data are consistent with the experimental findings. For the reaction of $GeAr'_2$ with H_2 the initial step is very similar. However there is just one intermediate (INT), in this case which transforms directly via TS2 or TS2′ to either Ar′GeH + Ar′H or Ar'_2GeH_2. The TS2 pathway leading to Ar′GeH + Ar′H has a slightly higher activation energy but has products that are thermodynamically more favored than Ar'_2GeH_2 by ca.19 kcal mol^{-1}. In this case it appears that the presence of the two large Ar′ groups introduces sufficient strain so that elimination of Ar′H is now preferred. The resulting monomeric Ar′GeH apparently reacts further with H_2 to form the $Ar'GeH_3$ product. The relative energies (Figure 5) of the ArGeH +ArH versus Ar_2GeH_2 (Ar = $Ar^{\#}$ or Ar′) reflect the steric pressure differences.

The initial pathways for the reaction of $SnAr^{\#}_2$ or $SnAr'_2$ with H_2 (Figure 8) are very similar to those described above for the germanium diaryls. Drawings of the intermediates and transition states are provided in Figure 9 and Figure 10. In both cases the energy pathways to the arene eliminated products are 7 and 4.7 kcal mol^{-1} lower than the oxidative additional pathway. In addition the arene eliminated product is always thermodynamically favored; by over 20 kcal mol^{-1} for Ar′SnH+ Ar′H and 6 kcal mol^{-1} for $Ar^{\#}SnH$ + $Ar^{\#}H$. Furthermore the dimerization energies of ArSnH (−21.6 kcal mol^{-1} for $Ar^{\#}$ and −20.0 kcal mol^{-1} for Ar′, see Supporting Information) make the eliminated pathway even more favored. These findings are in harmony with the experimental results which are the consequence of the increasing stability of the low oxidation state and larger size of tin versus germanium. However no reaction was observed between $SnAr^{\#}_2$ and H_2. This lack of reaction may be connected with the increased energy separation of the tin lone pair and p-orbital as indicated by the experimental and calculated values of λ_{max} as well as the HOMO−LUMO energy separations (Table 4).

(32) Kubas, G. J.; Ryan, R. R.; Swanson, B. L.; Vergamini, P. J.; Wasserman, H. *J. Am. Chem. Soc.* **1984**, *106*, 451.

The DFT calculations for the reactions of $GeAr^{\#}_2$ or $SnAr^{\#}_2$ with NH_3 indicate that the pathway involving a single NH_3 molecule had a high energy barrier in which no transition state could be located. Since excess NH_3 was used in the experiment, the alternative pathway involving the participation of a second NH_3 molecule was considered in the calculations. Calculated reaction pathways for the reactions of $GeAr^{\#}_2$ and drawings of the intermediates and transition state structures are provided in Figure 11 (those for $GeAr'_2$ are very similar). The initial step is the interaction of a lone pair on the nitrogen of an NH_3 molecule with the 4p or 5p orbital of Ge or Sn to form the intermediate (INT) $Ar^{\#}_2GeNH_3$ or Ar'_2GeNH_3 complexes. In the presence of excess ammonia, a second NH_3 molecule solvates the complexed NH_3 via intermolecular N--H interactions. The calculated structure of INT shows that the NH_3 complexed to germanium has a Ge−N distance of 2.073 Å. This value is very close to the 2.093(4) Å observed in the Ge(II) binaphthoxide ammine complex (*R*)-[Ge{$O_2C_{20}H_{10}(SiMe_2Ph)_2$-3,3′}{$NH_3$}].[33] The INT then transforms via either TS or TS′ to $Ar^{\#}H$ eliminated or oxidative addition product respectively. The oxidative pathway (TS′) is considerably (5.7 kcal mol^{-1}) lower in energy than the alternative elimination pathway even though the eliminated product $Ar^{\#}GeNH_2 + Ar^{\#}H$ is much more energetically favored than $Ar^{\#}_2Ge(H)NH_2$. The experimental findings showed that the kinetically favored $Ar^{\#}_2Ge(H)NH_2$ via TS′ is the only stable isolated product. The pathways for the reaction of $SnAr^{\#}_2$ with NH_3 (Figure 12) differs from that of $GeAr^{\#}_2$ in that the transition state TS and TS′ have almost identical energies, differing by only 0.4 kcal mol^{-1}. The oxidative addition product $Ar^{\#}_2Sn(H)NH_2$ is energetically disfavored by 2.2 kcal mol^{-1} whereas the $Ar^{\#}H$ eliminated divalent product $Ar^{\#}SnNH_2$ is strongly favored by 20.3 kcal mol^{-1}. The bulkier species $SnAr'_2$ behaved similarly and the $Ar'SnNH_2$ product is also strongly favored.

(33) Weinert, C. S.; Fanwick, P. E.; Rothwell, I. P. *J. Chem. Soc., Dalton. Trans.* **2002**, 2948.

Conclusions

The reactions of the $GeAr_2$ (Ar = $Ar^{\#}$ or Ar′) with H_2 or NH_3 invariably favor Ge(IV) addition products in contrast to their $SnAr_2$ analogues which yield arene eliminated Sn(II) products exclusively. The results show that electronic effects as manifested in lone pair stabilization are more important than the steric effects of those of the ligands.

Acknowledgment. The authors thank the U.S. Department of Energy Office of Basic Energy Science (DE-FG-02-07ER4675) for financial support. This work was also financially supported by the Grants-in-Aid for Creative Scientific Research, Scientific Research on Priority Area, and Next Generation Super Computing Project (Nanoscience Program) from the Ministry of Education, Science, Sports, and Culture of Japan.

Supporting Information Available: Crystallographic data for **1**, **2**, **3**, **5** (CIF), "de-twin" procedure for **2**, **3**, and **5**, dimerization energy for $Ar^{\#}SnH$ and Ar′SnH and full citation for ref 17. This material is available free of charge via the Internet at http://pubs.acs.org.

JA9068408